Biological auto(chemi)luminescence imaging of oxidative processes in human skin

Michaela Poplová,[†,‡] Ankush Prasad,[¶] Eduard Van Wijk,[§] Pavel Pospíšil,[¶] and Michal Cifra[*,‖]

[†]*Institute of Photonics and Electronics, The Czech Academy of Sciences, Prague, 182 00 ,Czechia*

[‡]*Faculty of Electrical Engineering, Czech Technical University in Prague, Prague 166 27, Czechia*

[¶]*Department of Biophysics, Faculty of Science, Palacký University, Šlechtitelů 27, 783 71 Olomouc, Czech Republic*

[§]*Meluna Research, Business & Science Park Wageningen, Agro Business Park 10, 6708 PW Wageningen, Netherlands*

[‖]*Institute of Photonics and Electronics, The Czech Academy of Sciences, Prague, 182 00, Czechia*

E-mail: cifra@ufe.cz

Phone: +420 266 773 454

Abstract

Oxidative processes present across all types of organisms cause the chemical formation of electronically excited species with subsequent ultra-weak photon emission termed biological autoluminescence. Thus, imaging of this luminescence phenomenon using ultra-sensitive devices potentially enables monitoring of oxidative stress in optically accessible areas of the human body, such as skin. Although most of the works

explored oxidative stress induced by UV light, for chemically induced stress, there is no quantified imaging of oxidative processes in human skin using biological autoluminescence under the controlled extent of oxidative stress conditions. Furthermore, the mechanisms and dynamics of the biological autoluminescence from the skin are not fully explored. Here we demonstrate that different degrees of oxidative processes on the skin can be spatially resolved through non-invasive label-free biological autoluminescence imaging quantitatively. Additionally, to obtain insight into the underlying mechanisms, we developed and employed a minimal chemical model of skin based on a mixture of lipid, melanin, and water to show that it reproduces essential features of the response of real skin to oxidative stress. Our results contribute to novel, noninvasive photonic label-free methods for quantitative monitoring of oxidative processes and oxidative stress.

Introduction

The mere fact that biological tissues generate endogenously electron-excited molecular species, which lead to luminescence even without any prior light stimulation[1] is fascinating and exciting. The major accepted mechanism that provides energy for the generation of excited states lies in chemical reactions initiated by reactive oxygen species (ROS).[2,3] Hence, this phenomenon is considered to be an endogenous biological auto(chemi)luminescence (BAL), often termed ultra-weak photon emission. The spectrum of this luminescence lies in the wavelength range of at least 350-750 nm, the integral intensity across this band is from 10 to 1000 photons$\cdot s^{-1}\cdot cm^2$ of the samples and is present at all levels of living species ranging from the simplest organisms such as bacteria up to humans.[1,4,5] Various stress factors can lead to an increase in ROS production[6,7] and consequently also increase BAL intensity.[8] In this paper, we explore imaging of various degrees of oxidation stress induced in vivo in human skin using BAL and in chemical model systems.

We provide first a brief overview of the general underlying mechanism of the BAL gen-

eration. Free radicals and reactive non-radical species chemically react with biomolecules, such as lipids, proteins, and DNA.[3] These reactions lead to the formation of unstable intermediates such as dioxetanes[9–11] and tetraoxides,[12,13] which in turn can decompose into electronically excited species, such as excited triplet carbonyl[14,15] or singlet oxygen.[16,17] The excited states can decay radiatively to generate a photon of BAL. Some molecules influence this reaction chain at the very beginning by either suppressing or promoting oxidation, hence the BAL generation. One of the molecules which is often at the initial part of the reaction chain is hydrogen peroxide (H_2O_2). H_2O_2 is generated endogenously in cells[18–20] and is also commonly used to induce oxidation when added to biological samples.[5,21–23] While H_2O_2 has a relatively low redox potential to oxidize most biomolecular directly (apart from a few selected group such as sulfhydryls[24,25]), it can participate in Fenton or Haber-Weiss reaction[26–29] to produce the hydroxyl radical, which is the most potent biologically relevant radical able to oxidize virtually any biomolecule. Typically, only trace amounts of reduced transition metal cations (Cu^+, Fe^{2+}) are sufficient to generate hydroxyl radicals from H_2O_2. Hydroxyl radical or other primary radicals produced can then initiate chain reaction, which is manifested as autooxidation.[30]

What are the typical characteristics of BAL from humans? The BAL from human subjects in vivo has been acquired so far only from the outer surface of human body,[31–35] which is mostly covered by skin. There, it is the upper layer of skin that is involved in emitting BAL from the human body.[36] The general findings are that the BAL intensity depends on a variety of factors,[34] including a particular site of the body cite,[37] physical activity,[38,39] displays anatomic asymmetry,[40,41] undergoes diurnal, monthly and annual cycles,[42–46] tends to increase with age[47] and together with spectral analysis has the potential to monitor disease processes, such as diabetes, hemiparesis, protoporphyria, or a typical cold.[4] Although systemic and internal states of the human body influence the processes in the skin, on the human body scale, there is evidence that BAL signals originate from the upper layers of skin.[48] For this reason, BAL works on humans are often related to skin research and der-

matology, reporting the capability of BAL to report on oxidation processes in the skin.[49,50] Currently, there are two methods used for the measurement of BAL. Temporal patterns of BAL by a highly sensitive photomultiplier tube and spatial distribution (imaging) of BAL by a cooled CCD camera, which was used in this study. For both methods, it is necessary to ensure measuring conditions without the presence of external light and take measures against delayed luminescence.[1,33,51] While most of the BAL research employs single-channel photomultipliers as the main workhorse for BAL detection,[1] the imaging of BAL brings a substantial advantage for the BAL research of spatially structured systems such as skin.

Imaging naturally provides spatial information of BAL from skin.[41,52] The skin protects humans against continuous oxidative damage by ROS coming from environmental stresses (physical and chemical factors).[36,53] Imaging spontaneous BAL from different parts of the human body[37] has been employed in the past and uncovered temporal variations of BAL,[43] the influence of oxygen content in the environment[54] or effect of scavengers.[53,54]

While it already has been demonstrated using sensitive CCD cameras that H_2O_2[36,53] or other oxidizing treatments such as UVA[53] elicits increased UPE from human skin, the possibility to spatially discern oxidative stress of various defined degrees within a single image in vivo has not been demonstrated yet.

The relation of BAL to oxidative stress has been previously reported in several studies. The main benefit of this direct measurement of BAL in the skin is that it can also be measured in vivo under physiologically relevant conditions. During the last few decades, BAL measurements (also called low-level chemiluminescence, biophotons, etc.) have been performed on skin either in biopsies (ex vivo skin models),[48,55,56] in vivo and in vitro conditions (keratinocytes, fibroblast, homogenate, etc.) under diseased conditions such as malignancy and/or externally applied stresses (such as ultraviolet irradiation, exogenously applied chemicals).[48,57–62] The studies mentioned above concluded that BAL can be used as methods for evaluating the physiology of the skin and helping to understand how skin tissues react to different exogenous stresses. Therefore, it has been claimed that BAL can be used as a

signature for oxidative radical reaction in skin and therefore can serve as a tool for understanding skin conditions related to free radicals, such as wound healing, skin aging (which occurs principally by breaking down skin collagen), skin cancer among others. There are often challenges related to the measurement of BAL in skin, the primary reason being the low intensity of BAL. However, the intensity of BAL has been shown to increase by several folds in the case of the application of various (oxidative) stimuli.[48,63] In most studies, the increase in BAL emission is claimed to be related to free radical generation; however, there is little evidence on the mechanism of how these phenomena are linked.

In this work, we use an ultra-sensitive EMCCD camera-based system to image the spatial distribution and photomultiplier system to detect the kinetics of biological autoluminescence from human skin from the chemical model system. Using both of these techniques, we test the capability of quantitative differentiation between several degrees of oxidation level induced by the application of hydrogen peroxide and the possibility of monitoring the protective effect of antioxidants. Our study also addresses the issue of underlying mechanisms on a chemical model system by validating the ROS-based mechanism of BAL generation using electron paramagnetic spin (EPR) trapping spectroscopy and high-performance liquid chromatography (HPLC), where the chemical skin content was mimicked with a pigment (melanin), lipids (linoleic acid), and water.

Experiment and methods

Measurement equipment

Luminescence measurements were performed in light-tight black chambers (custom-made by the Bioelectrodynamics research team, Institute of Photonics and Electronics of the Czech Academy of Sciences) which have light-proof sleeve designed for direct access to the interior chamber without any light leakage. Both setups are depicted in Figure 1.

For the luminescence imaging, the highly sensitive Andor iXon ULTRA 888 back-illuminated

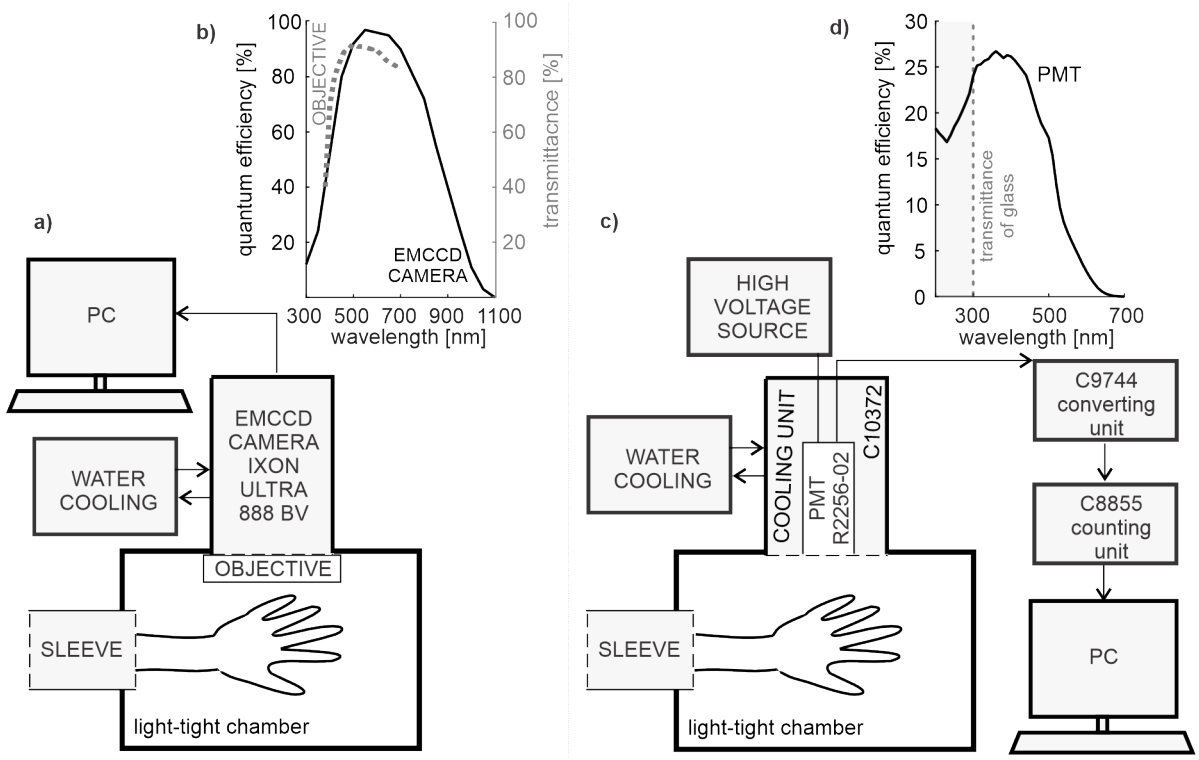

Figure 1: Scheme of measurements for a) spatial distribution (imaging) and c) temporal distribution (kinetics) of BAL. The same setups were used both for experiments with hand and chemical model system (Petri dish) b) shows QE of EMCCD camera and transmittance of objective lenses. d) shows the QE of the PMT detector, where we also display the transmittance limit of the PMT input window (borosilicate glass).

electron-multiplying charge-couple device camera (EMCCD, Andor Technology Ltd, 118 Belfast, Northern Ireland) with a Xenon 0.95/25 mm objective (Jos. Schneider Optische Werke GmbH, Bad 131 Kreuznach, Germany) was mounted on the top of the black chamber (Figure 1a). The spectral response of the EMCCD is in the range 300–1100 nm with the peak quantum efficiency 97.5 % at 575 nm (Figure 1b). The objective with a maximum relative aperture 0.95 is perfectly suitable for low light conditions and its transmittance is designed for visible spectrum from 400 to 700 nm (Figure 1b). The EMCCD detector was cooled to -100 °C by thermoelectric cooling system supplemented with an extra water cooling chiller (OasisTM 160LT, Solid State Cooling Systems, 126 NY, USA) for dark current reduction. Each luminescence image was obtained by following setting: 4 × 4 binning, 16 bits at 1 MHz readout rate, 1024 × 1024 pixel format, 1.7 s vertical shift speed, 'normal' clock amplitude, electron multiplying gain level 300, pre-amplifier gain 5.2. The distance between the detector and sample was approximately 30 cm.

The time series of BAL were measured by the photomultipler R2256-02 (PMT, Hamamatsu Photonics Deutschland, DE) see in Figure 1c. This head-on type PMT has a circular photocathode with 46 mm diameter and its sensitivity is in the wavelength range from 160 to 650 nm with the peak of sensitivity at 420 nm (Figure 1d). The PMT was cooled inside the housing unit C10372 (Hamamatsu Photonics Deutschland, DE) to -30 °C with the support of water cooling and powered at -1550 V by high voltage power supply PS350 (Stanford Research System, USA). The pulses from PMT were amplified and converted to TTL pulses by the unit C9744 (Hamamatsu Photonics Deutschland, DE) and processed by counting unit C8855 (Hamamatsu Photonics Deutschland, DE) connected to computer (PC).

EPR and HPLC methods

The following methods were used to analyze the oxidative processes in the chemical model system. We used electron paramagnetic resonance (EPR) for a sensitive detection of sub-

stances with unpaired electrons, i.e. radical species. In our case, we focused on the formation of $^1O_2$ in model system. EPR signals were measured by spectrometer MiniScope MS400 (Magnettech GmbH, Berlin, Germany). As a spin label, we used a hydrophilic diamagnetic TMPD (2,2,6,6-tetramethyl-4-piperidone, Sigma Aldrich GmbH, USA) which produced paramagnetic 2,2,6,6-tetramethyl-4-piperidone-1-oxyl (TEMPONE) in presence $^1O_2$ which gives EPR signal. TMPD was purified twice by vacuum distillation to reduce impurity from TMPD EPR signal. The reaction mixture was treated and transferred into a glass capillary tube and EPR spectra were collected at room temperature. Incubation time was 10 min. Signal intensity ($r.u.$) was calculated from the first peak of EPR spectrum. EPR spectrometer settings were as follows: microwave power 10 mW; modulation amplitude 1 G; modulation frequency 100 kHz; sweep width 100 G; scan rate 1.62 G$\cdot$s^{-1}.

We used high-performance liquid chromatography (HPLC) to separate and identify oxidative products. In our model system, we monitored the amount of malondialdehyde (MDA) which is an indicator of oxidative stress as a product of lipid peroxidation. MDA reacted with 2,4-dinitrophenylhydrazine (DNPH) in the creation of 2,4-dinitrahtdrazine (MDA-DNPH). Detection of MDA-DNPH adduct was performed by a reversed-phase high-performance liquid chromatography (HPLC) using Alliance e 2695 HPLC System (Waters, Milford, MA, USA) equipped with 2998 Photodiode Array detectors for UV-VIS absorption detection. The isocratic separation was carried out using a LiChrosper 100 RP-18 (5 um) LiChroCART 250-4(Merck, Darmstadt, Germany) with acetonitrile:water (50:50 v/v) as a solvent system and a flow rate of 0.5 ml min-1.

Subject

A healthy volunteer (the first author, female, age 29, skin type III) participated in this study following the ethical standards in the Declaration of Helsinki. Before measurement, the hand was washed with antibacterial unscented soap and water. We have not observed any effect

of this washing treatment on BAL signals. After this procedure, the hand was placed into a light-tight chamber for 30 minutes to prevent delayed luminescence. BAL was measured from the dorsal side of the right hand in each experiment: 20 minutes for BAL kinetics detection using PMT and 30 minutes for BAL imaging using EMCCD camera.

Model system of skin

The proposed minimal chemical model of the skin is composed of linoleic acid (Sigma-Aldrich, L1376) that here serves as a model lipid, melanin (Sigma-Aldrich, M8631) as a model pigment that plays an important role in the oxidation reactions and Fe^{2+} ($FeSO_4 \cdot 7H_2O$, P-LAB, R.P015.1) as an initiator of the Fenton reaction. Model sample was prepared without mixing and their total volume was 3 mL (fractions: 0.3 mL H_2O or Asc^+, 2 mL lipid stock solution, 0.2 mL melanin stock solution, 0.2 mL iron stock solution, 0.3 mL H_2O_2 stock solution). The final concentrations of chemicals are provided in Table 1. Linoleic acid was dissolved in physiological saline - 0.9 % NaCl(sodium chloride, Penta, 16610-31000) together with 0.7 μM DMSO (dimethyl sulfoxide, P-LAB, 12630-11000). Linoleic acid provides a substrate for the lipid peroxidation process in a model system. Melanin was dissolved in DMSO. Melanin is one of the major cutaneous pigment. Micromolar to millimolar concentrations of iron cations are present in biological systems.[64–66] The reactions of Fe^{2+} and other transition metals with hydrogen peroxide (H_2O_2) lead to the Fenton and Fenton-like reactions which initiate radical oxidation of organic molecules either via generated hydroxyl radical ($HO^\bullet$) or other pathways.[67]

Chemical treatment

Two different studies were conducted, the first on varying degrees of oxidative stress (by varying the concentration of hydrogen peroxide) and the second on antioxidant effects in samples. For the first study, we used hydrogen peroxide (Penta, 23980-11000) with three different final concentrations (c_1=3 %, c_2=0.9 %, c_3=0.3 %), where 0.3 mL stock solution was

Table 1: Final concentration of chemicals in experiments with model system

	PMT/EMCCD	EPR[a]	HPLC
linoleic acid	10 mM	10 mM	10 mM
melanin	0.15 mM	0.15 mM	-
Fe^{2+}	2 mM	2 mM	2 mM
H_2O_2	3/0.9/0.3 %	0.3/0.09/0.03 %	0.09 %
	$\sim$ 880/264/88 mM	$\sim$ 88/26.4/8.8 mM	$\sim$ 26.4 mM
Asc^+	5 mM	5 mM	-

[a] 25 mM TMPD (spin trap) added ;

injected. For testing the protective effect of antioxidants on skin we used ascorbic acid (AA, Penta, 18650-30500) with 5 mM final concentration, it was used 0.3 mL of stock solution. For antioxidant experiment, oxidative stress of the skin was induced by 3 % hydrogen peroxide which increased BAL. The chemical model system was in plastic Petri dish (35 mm diameter, Thermo Scientific, Nunc cell culture/Petri dishes) without a lid for the experiments.

For imaging experiments on the skin, three rectangular spots were defined by a mask from transparent adhesive tape and black dots. Each substance of volume 5 μL was applied by micropipette and the drop was uniformly distributed by gloves in each rectangular spot. After these procedures, the tape mask was removed prior to measurement. The gray scale image of the hand was taken after each luminescence imaging experiment. For antioxidant experiment, we first applied the first ascorbic acid and then the H_2O_2. For the BAL measurement with PMT, experiments with each concentration were carried out consecutively. There, in experiments with a hand, a given substance (10 μL) was applied on the whole area of the dorsal side of the hand, in contrast to the imaging experiments, where only smaller limited areas were treated.

Data processing

Raw PMT signals were fitted by function smoothn.m[68 69] designed by D.Garcia with parameter 'robust' which minimizes the influence of outlying data (see in Figure 2). This smoothing method is based on discretized spline with the minimization of the generalized

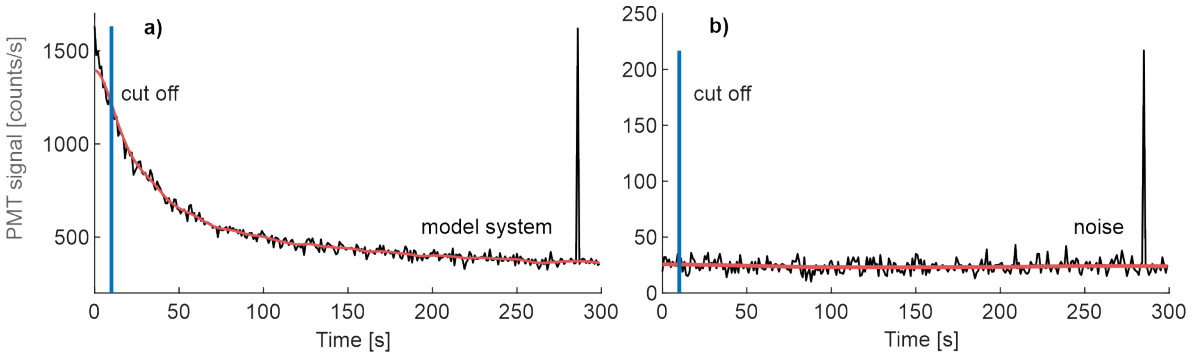

Figure 2: Preprocessing of PMT signals was composed from smoothing the signal (red line) and their shortening from blue cut-off line. The red shortened smoothed signals were used for next analyses. In picture is shown typical BAL signal of chemical model system a) black line and noise of PMT b) black line.

cross-validation score. Due to estimation error in the beginning of signal (see in Figure 2a) the first 10 values were removed (blue vertical line). These smoothed shortened lines were used for further data analysis.

Imaging data were recorded by Andor Solis software in SIF format. Original images have 256 × 256 pixels due to software binning 4 × 4 and grey scale from 0 to 65535 intensity levels. The image was converted to .dat format for analysis by Matlab software.[70] Data included noise which distorted the results of the analysis. The preprocessing method was based on thresholding. We calculated a cumulative sum from the histogram of image and empirically determined the threshold of 99.6 % for hand and 99.8 % for model system. The values equal to or higher than the threshold were replaced by NaN values, which were not included in the further analysis. Figure 3 shows the whole image processing procedure.

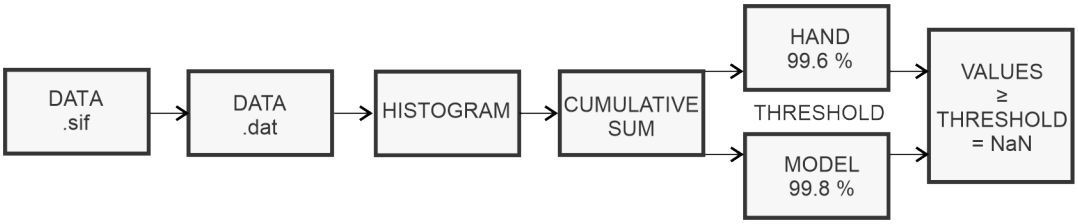

Figure 3: Scheme of preprocessing procedure for the quantitative analysis of the image data. The thresholding was used to remove the outliers and excessive noise, see the text for a detailed description.

Results and discussion

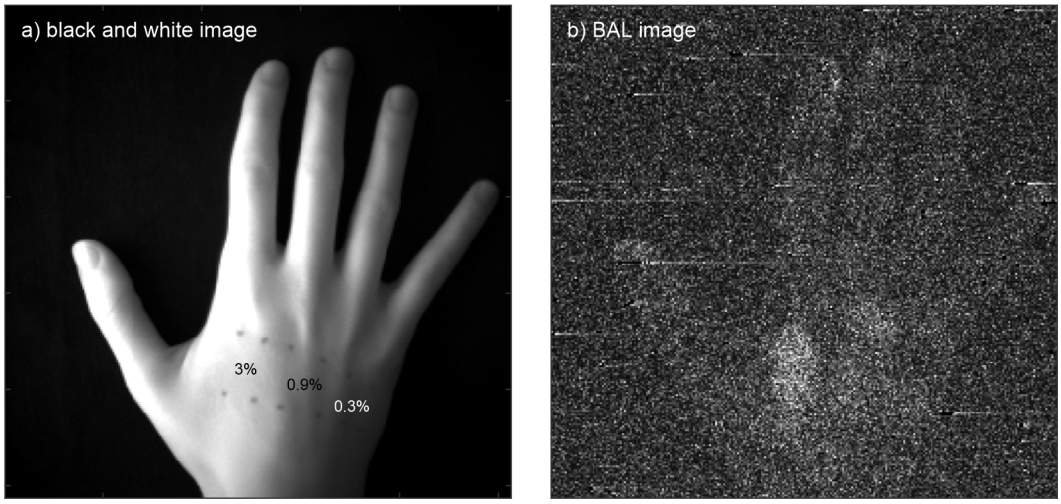

Figure 4: A typical a) the greyscale image of a hand and the corresponding b) BAL image from EMCCD camera. The four dots mark the corners of rectangular sites where the c_1=3 %, c_2=0.9 %, c_3=0.3 % concentration of hydrogen peroxide was applied on the skin.

Biological autoluminescence: imaging and kinetics

To test whether BAL imaging can be used to quantify the spatially heterogeneous distribution of oxidative stress, we performed a parallel topical skin treatment with H_2O_2 concentration row (c_1=3 %, c_2=0.9 %, c_3=0.3 %) on the selected sites on a dorsal side of the right hand of the test subject (Figure 4a). The BAL from the skin (Figure 4b) was imaged for 30 min using cooled EMCCD camera (Andor iXon3 888) mounted to our custom-built light-tight chamber. While the endogenous BAL signal from the skin is only weakly above the dark count the BAL image following the shape of the hand is clearly discernable.

We show a representative image of BAL from the human hand with three topical H_2O_2 treatments in Figure 5a. Apart from endogenous BAL, which follows the morphology of the hand, it can be seen that the higher the concentration of H_2O_2 (higher oxidative stress) the higher the BAL intensity from the topically treated skin areas. Beyond the three major areas of interest, where the H_2O_2 was applied, one can notice patches of increased BAL intensity. The most prominent one in the current Figure 5a is at the root of the thumb and there seem

to be several other smaller ones scattered on the hand. It cannot be excluded that the small patches are just due to instrumental noise. However, the larger patch likely does correspond to light emitted from the skin and is of unknown origin. Patches of comparable or even larger are not uncommon in the imaging of BAL from the human hand[46] even if great care is taken to avoid skin treatments. They might indicate local skin irritation due to a variety of factors and subclinical skin conditions which are not visible by visual observation by a naked eye. A systematic study would be required to find a causal relationship of the origins of the patches.

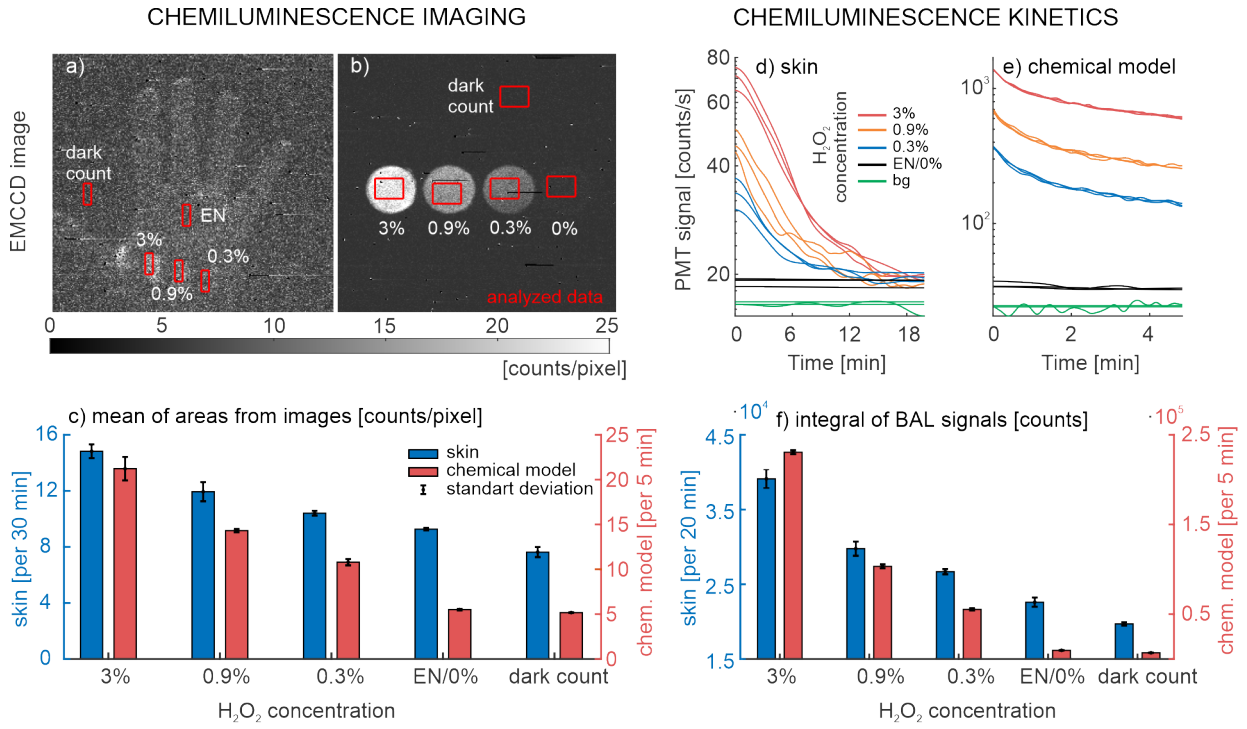

Figure 5: Different degrees of H_2O_2 oxidation induced biological auto-luminescence (BAL) of skin and chemical model system in the temporal and spatial distribution. Mean values and standard deviations are from N=3 independent experiments. In the BAL image of hand a) red rectangular analyzed areas with identical area were used for the analysis across all hand BAL measurements. Three different concentrations of hydrogen peroxide were applied on the skin (3 %, 0.9 %, 0.3 %) and also endogenous (EN) BAL signals as well as a dark count of the detector were captured. The same approach was used in BAL images of chemical model system - there the label 0 % corresponds to with the vehicle (Q-water) only applied. c) shows mean values of analyzed areas from hand (left axis: blue bars) and chemical model system (right axis: red bars). The smoothed kinetic BAL signals from skin d) and chemical model system e) are evaluated in f) as the integral sum of BAL from skin (left y-axis: blue bars) and chemical model system (right y-axis: red bars).

In this work, we focused on the BAL signals from the sites of topical H_2O_2 treatment of skin (Figure 5a) and quantified the imaging data. Our quantified results in Figure 5c (left y-axis: blue bars) display mean values from the three skin areas treated by different concentrations of H_2O_2 as well as from non-treated skin area, all from three experimental replicates. The BAL signal intensity increases with increasing H_2O_2 concentration. While the endogenous BAL signal (0 % H_2O_2) from the skin is around 1.5 counts/pixel, it increases to ca. 6.5 counts/pixel for 3 % H_2O_2, above the mean of the dark count (ca 8 counts/pixel). These results demonstrate that BAL imaging is able to discern different levels and spatial distribution of oxidative treatments and stress on the skin.

Inspired by Kobayashi,[71] we developed a well-defined minimal chemical model system of the skin: water solution of linoleic acid and melanin (see methods for details). We selected linoleic acid[72] as a representative of the 16 and 18 carbon-free fatty acids which are together with triglycerides the major (57.5 %) component of skin surface lipids,[73] and melanin as a pigment important in skin photophysical and photochemical processes. Linoleic acid is also a suitable model in oxidation experiments since it is a polyunsaturated fatty acid containing two double bonds which make it prone to oxidation attack.[75] To induce the oxidation in a chemical model (Figure 5b - 3 mL in a Petri dish), we used the same H_2O_2 concentration row (0.3 %, 0.9 %, 3 %) as in the skin. The image clearly shows that the BAL signals are much higher than the background and depend on the H_2O_2 concentration. The quantified results in Figure 5c (right y-axis: red bars) display mean values from specific areas from two replicate measurements. They show that the H_2O_2 elicits increased BAL intensity in a chemical model in a concentration-dependent manner with a behavior qualitatively similar to the response of BAL from hand, albeit with higher intensities. There are at least these four major differences in the chemical model in contrast to the skin which contribute to the higher overall BAL signal from the chemical model than from skin:

- higher volume of H_2O_2 added to the chemical model than on the skin sample: 300 μL vs. 5 μL on the whole dorsal side of the hand

- in liquid, in contrast to a solid skin surface, the diffusion is much faster
- the exact chemical composition of the skin is different from the chemical model which contains just representative molecules of lipids and pigments
- there is no antioxidative system in the chemical model

To analyze kinetics of BAL from skin, we used our sensitive photomultiplier tube (PMT) system. Three concentrations (0.3 %, 0.9 %, 3 %) of H_2O_2 has been applied consecutively on the whole dorsal side of the right hand of the test subject. The results are in Figure 5d. The endogenous BAL signal was approximately 3 counts/s (the background (PMT dark count) was around 16 counts/s). H_2O_2 treatment induces a substantial increase of BAL intensity in a concentration-dependent manner, with 3 % treatment causing approximately more than a 15-fold increase of net BAL at the time=0 of the measurement. Using the PMT detection technique, we were also able to follow the kinetics of BAL after H_2O_2 treatment in both hand (Figure 5d) and its chemical model (Figure 5e). After H_2O_2 treatment, the BAL intensity from the skin decays to the level of endogenous BAL within 12-19 min (Figure 5d) depending on amount of H_2O_2. In the case of chemical model, BAL intensity drops to approx. 38-44 % of the H_2O_2 induced value within 5 min, yet still being almost one order of magnitude higher than the spontaneous BAL. We suggest the following explanation of the differences between the kinetics of the decay of BAL between the skin and chemical model: The skin possesses an antioxidative system that is activated after oxidative insult to remove excessive reactive oxygen species, as known in other tissues.[76] However, the chemical model treated with H_2O_2 experiences an initiation of chain lipid peroxidation[77] which can persist for an extended period of time with no antioxidants to terminate the propagation. In general, the integral value of H_2O_2 concentration-dependent BAL signals scales similarly both for imaging (Figure 5c) and kinetics data (Figure 5f) confirming the validity of the data. How does the intensity of BAL induced due to oxidative stimulus relates to endogenous BAL? This question boils down to the rate of the processes which lead to electron-excited state generation and photon

emission and the effective volume where these processes take place. The processes leading to photon emission in the skin are likely more complex than just the assumed Fenton reaction-based generation of ROS, which is dependent on % H_2O_2 and iron cations concentration. Nevertheless, for simplicity, let us discuss endogenous versus stimulated BAL intensity values and H_2O_2 concentrations. The integral BAL intensity from imaging data has a mean value of 1.6 and 7.2 counts/pixel for endogenous and 3% H_2O_2 stimulated cases, respectively, above the dark count, which had a mean value of 7.6 counts/pixel (Figure 5c). The concentrations of H_2O_2 we used were 880 mM, 264 mM and 88 mM. It is known from liquid chemical models from our earlier work that for fixed Fe^{2+} decreasing the concentration of H_2O_2 by an order of magnitude causes only 1.1–2-fold decrease of the integral BAL intensity, depending on a specific iron and H_2O_2 concentration.[78] In our case of BAL skin data, there is a 2.6-fold decrease of integral BAL intensity per one order of magnitude decrease of H_2O_2 concentration (from 7.2 counts at 3% H_2O_2 to 2.8 counts at 0.3% H_2O_2). If we extrapolated this value and decreased the BAL intensity (at 0.3% H_2O_2) 2.6-fold to correspond to 0.03% (88 mM) we would obtain the value 1.07 counts per pixel which is lower than the BAL value of 1.6 counts per pixel for non-treated skin (0% H_2O_2). However, the endogenous and biologically relevant steady-state values for intra-tissue H_2O_2 concentration lie in nM–μM range.[18,20,79]

How can we explain this seeming discrepancy? At first, the exogenously added H_2O_2 of the given concentrations was applied not to the whole accessible volume of the skin tissue, but on the surface of the skin only and the concentrations were only transient to simulate oxidative stress. The excessive H_2O_2 is then rapidly depleted (see Figure 5d). Another possible reason is that the BAL due to topically applied H_2O_2 is likely emitted only from a very thin layer (few microns) of upper layers of the skin, while the endogenous BAL is generated by a volumetric source - skin tissue. All other things being the same, the larger volume the higher BAL intensity. The quantitative answer to the question "What is the thickness of this volumetric source ?" is roughly bounded by the depth of the light penetration from/to the tissue. This very much depends on the wavelength of the light. The

BAL spectrum from the skin is rather broad with a peak at around 600 nm.[71] The models of light penetration to skin predict that light fluence decreases to about 50% of its original value at the surface of the skin at a few tens of 10 μm and around 1 mm in the skin for 400 nm and 600 nm wavelength, respectively, for a diffuse light source,[80] which is a good approximation of BAL. The reciprocity of light propagation suggests that these (10 μm–1 mm) are the depths in the skin from which we can expect the BAL reaches the surface and then also the photodetector.

After we showed that the BAL signal responds to oxidative treatment in a dose-dependent manner, we asked if our technique is capable of monitoring the protective effect of antioxidants. Antioxidant ascorbic acid was applied into the hand/model system as a prevention against oxidative effects of H_2O_2 which was added thereafter. As in the previous section, both EMCCD and PMT systems were used for BAL detection. Analysis of EMCCD images for both hand and model system (Figure 6a,b) supports the fact that antioxidant suppressed the oxidative effect of H_2O_2 see in Figure 6c: blue (skin) and red (model system) bars. While it was possible to distinguish the differences in BAL intensity in the previous experiment with various concentrations of H_2O_2 even by visual observation Figure 5a, the differences are more subtle in the case of antioxidant action (Figure 6a). The quantitative analysis showed that the BAL signal induced by 3% H_2O_2 is only slightly suppressed by ascorbate acid (Figure 6d). The BAL kinetics measurement using PMT uncovers the subtlety of this effect (Figure 6d: blue lines) the suppressing effect of ascorbic acid is only temporary, acting up to approximately 15 min. After this period, the signals with and without antioxidant are almost identical, see Figure 6d: red lines. It could be caused by the consumption of applied antioxidant. The ascorbic acid effect in the chemical model system (Figure 6e: blue lines) copies the trend of PMT signal without antioxidant (Figure 6e:red lines) but is approximately 200 counts lower across all the time. The analysis of the integral BAL of both systems (skin and chemical model) supports the assumption that ascorbic acid scavenges ROS, hence causes a decrease of BAL intensity (Figure 6f:blue (skin) and red (chemical

model) bars). These results are corroborated by earlier works where the application of variety of antioxidants including the ascorbic acid decreased BAL signal to a different extent.[48,54,63,81] Ascorbate, glutathione, α-tocopherol and coenzyme-Q were able to suppress even the intensity of endogenous BAL signals from human skin in vivo[54] and ascorbate also suppressed H_2O_2-induced signals from porcine skin in vitro.[48] Ascorbate, glutathione, and δ-tocopherol also mildly suppressed BAL increased by UV-induced reactive oxygen in human skin in vitro.[63]

Next, we aimed to dissect the lipid (linoleic acid) and pigment (melanin) contribution to the observed BAL signals. To do this, we varied the concentration of either linoleic acid or melanin in the chemical model system and induced the oxidation by treatment of Fe^{2+} and H_2O_2. The strategy was to start with equimolar lipid (linoleic acid) and pigment (melanin) concentration, keep the concentration of one component fixed and test the systems with gradually decreased concentration of the other component. See the details of concentrations in Table 2 and the results in Figure 7a, b. We found that the changes in BAL signals intensity caused by the different concentrations of LA (10 mM and lower, fixed 10 mM melanin) are minimal (Figure 7a). However, decreasing melanin concentration (0.15 mM and lower, fixed 0.15 mM melanin and lower) has a substantial effect on BAL intensity. Hence, we conclude that the most important modulating parameter of BAL signals for our chemical model system is melanin (Figure 7b).

Table 2: Final concentration of chemicals in sensitivity analysis of model system

sensitivity to:	linoleic acid	melanin
linoleic acid	0/0.1/10 mM	10 mM
melanin	0.15 mM	0.0325/0.075/0.15 mM
Fe^{2+}	2 mM	2 mM
H_2O_2	3 % $\sim$ 880 mM	3 % $\sim$ 880 mM

What could be some of the underlying ROS and excited-electron species leading to BAL ? Earlier works suggest that it is the triplet excited carbonyl and bimolecular emission of singlet oxygen, which are considered the main primary electron excited species leading to

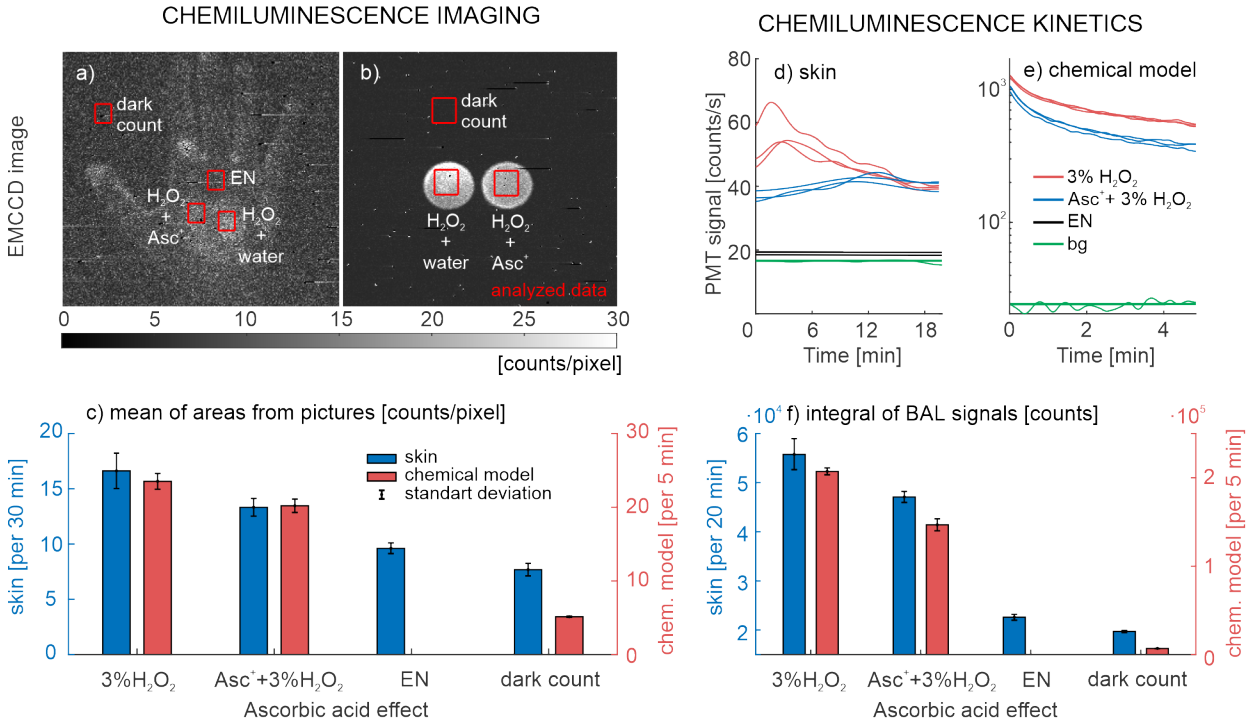

Figure 6: Antioxidant (ascorbic acid) suppresses the BAL signal induced by H_2O_2 treatment. In imaging of hand a) and chemical model system c) red rectangular areas are investigated: with or without ascorbic acid, endogenous BAL, and dark count which are analyzed in c) as mean values of skin (left y-axis: blue bars) and chemical model system (right y-axis: red bars). Preprocessed kinetic signals from skin d) and chemical model system e) are analyzed as an integral sum of BAL f) of skin (left y-axis: blue bars) and chemical model system (right y-axis: red bars).

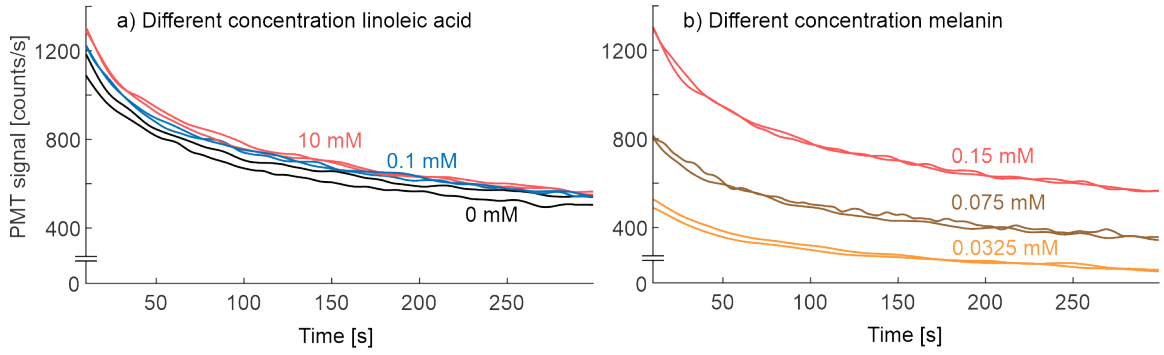

Figure 7: BAL kinetics data from a chemical model system for different concentrations of linoleic acid and melanin. The part a) shows data with varied linoleic acid concentrations (10 mM, 0.1 mM, and 0 mM) for fixed melanin concentration (0.15 mM) and b) shows data for varied concentrations of melanin (0.15 mM, 0.075 and 0.0325 mM) for a fixed linoleic acid concentration (10 mM).

BAL.[3] To understand this better in a controlled way, we focused on a chemical model system. Due to the multiple roles of singlet oxygen ($^1O_2$), being both ROS and potential emitter, we decided to focus on this specie. We used spin-trapping electron paramagnetic resonance (EPR) spectroscopy to confirm the presence of $^1O_2$ emerging in our chemical model system. One data set of TEMPONE EPR spectra (10 min incubation and measurement) is shown in Figure 8a: color lines. The bar graph result shows that the (max - min) value from the first peak in EPR signals (three replicates) (Figure 8a: bars) decreases with decreasing concentration of H_2O_2 (0.3 %,0.09 %, 0.03 %, 0 %). For this experiment, we used a 10-fold lower concentration of H_2O_2 considering the sensitivity of spin-trapping EPR spectrometry. The characterization of the relative EPR signal is more than sufficient for spin trapping procedures and using higher concentration may lead to oversaturation of signal intensity. We also performed a control experiment, where the effect of Fenton's reagent containing 0.3% H_2O_2 was tested on a sample without melanin according to previous sensitivity analysis of a model system (Figure 7a, b). Removal of melanin led to partial suppression of EPR signal (data not shown). The application of antioxidant ascorbic acid into chemical model system led to the significant reduction of $^1O_2$ (Figure 8b: bars) and the formation of monodehydroascorbate radical (Asc^-).

Further, HPLC method was used for confirmation of the presence MDA as a product of lipid peroxidation in our model system. Figure 8c shows chromatogram of Fenton reagent-treated linoleic acid with the peak of MDA-DNPH adduct at retention time of 25.2 min. The absorption spectrum of MDA-DNPH adduct shows maximum at 325.2 nm (data not shown).

Conclusion

Via detection and analysis of biological auto(chemi)luminescence (BAL), we demonstrate the capability of quantitative differentiation between several degrees of oxidation level on

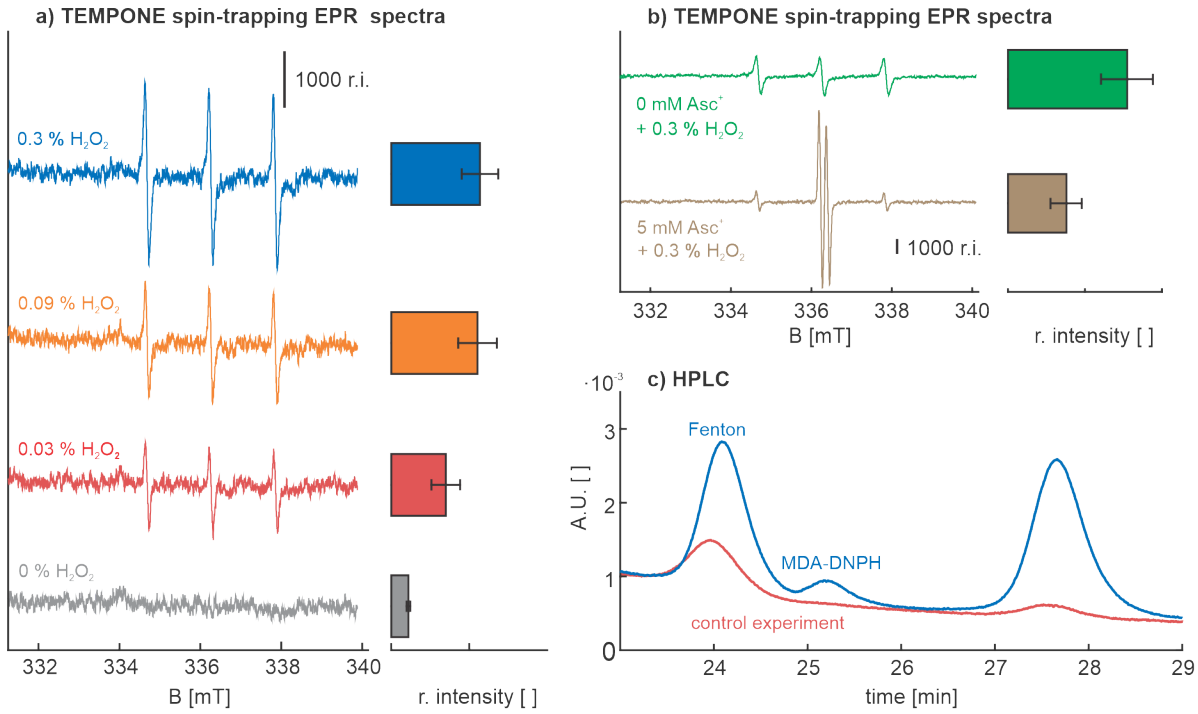

Figure 8: a) EPR signals of different H_2O_2 concentrations from chemical system (left side:lines) and mean values from max-min value of first peak (right side:bar graphs); b) EPR signals from chemical model system of 0.3 % H_2O_2 with and without ascorbic acid (left side:lines) and their mean values from max-min value of first peak (right side: bar graph); c) Chromatograms of MDA-DNPH adduct detected by HPLC in control experiment (10 mM Linoleic acid) is represented by a red line and chemical model system without Melanin is represented by a blue line. See details of concentrations in Table 1.

human skin in vivo induced by the application of hydrogen peroxide and the possibility of monitoring protective effect of antioxidants. In our work, it is for the first time we quantitatively demonstrated topical differences due to chemically-induced oxidative stress within one image in human in vivo. This is very important because the variability between subjects, their physiological states, skin types and conditions, and different imaging systems and settings has not been fully described. Using the imaging (EMCCD) technique of BAL we demonstrated not only quantitative difference but also the capability of identifying spatial inhomogeneity and local differences of oxidative stress under controlled conditions. For data analysis, we also developed a semi-automatic method for processing and analysis of the BAL images from CCD camera. The data from BAL correlated well with the minimal chemical model of skin. In this experimental model, we showed that the content of pigment (melanin) has a strong role in the overall BAL signal. Using spin trapping EPR spectroscopy, we detected the presence of singlet oxygen, which is both a potential emitter of BAL as well as a reactive oxygen specie itself. The oxidation in the samples was confirmed by the detection of malondialdehyde as a product of lipid peroxidation. Overall our results demonstrate that BAL is a label-free, real-time, in-situ, non-contact, non-invasive, and probably the only technique which requires no acute external energy input to the biosystem to observe the oxidation processes.

Acknowledgement

MC and MP acknowledge Czech Science Foundation project no. 20-06873X. AP and PP were supported by the European Regional Development Fund project *Plants as a tool for sustainable global development* (CZ.02.1.01/0.0/0.0/16$_0$19/0000827).

References

(1) Cifra, M.; Pospišil, P. Ultra-weak photon emission from biological samples: Definition, mechanisms, properties, detection and applications. *Journal of Photochemistry and Photobiology B: Biology* **2014**, *139*, 2–10.

(2) Pospíšil, P.; Prasad, A.; Rác, M. Role of reactive oxygen species in ultra-weak photon emission in biological systems. *Journal of Photochemistry and Photobiology B: Biology* **2014**, *139*, 11–23.

(3) Pospíšil, P.; Prasad, A.; Rác, M. Mechanism of the Formation of Electronically Excited Species by Oxidative Metabolic Processes: Role of Reactive Oxygen Species. *Biomolecules* **2019**, *9*, 258.

(4) Zapata, F.; Pastor-Ruiz, V.; Ortega-Ojeda, F.; Montalvo, G.; Ruiz-Zolle, A. V.; García-Ruiz, C. Human ultra-weak photon emission as non-invasive spectroscopic tool for diagnosis of internal states – A review. *Journal of Photochemistry and Photobiology B: Biology* **2021**, *216*, 112141.

(5) Vahalová, P.; Cifra, M. Biological autoluminescence as a perturbance-free method for monitoring oxidation in biosystems. *Progress in Biophysics and Molecular Biology* **2023**, *177*, 80–108.

(6) Halliwell, B.; Cross, C. E. Oxygen-derived species: their relation to human disease and environmental stress. *Environmental Health Perspectives* **1994**, *102*.

(7) Ghaemi Kerahrodi, J.; Michal, M. The fear-defense system, emotions, and oxidative stress. *Redox Biology* **2020**, *37*, 101588.

(8) Van Wijk, R.; Van Wijk, E. P. Free radicals and low-level photon emission in human pathogenesis: State of the art. *INDIAN J EXP BIOL* **2008**, 37.

(9) Cilento, G. Generation of electronically excited triplet species in biochemical systems. *Pure and Applied Chemistry* **1984**, *56*, 1179–1190.

(10) Cilento, G.; Adam, W. Photochemistry and photobiology without light. *Photochemistry and photobiology* **1988**, *48*, 361–368.

(11) Velosa, A. C.; Baader, W. J.; Stevani, C. V.; Mano, C. M.; Bechara, E. J. H. 1,3-Diene Probes for Detection of Triplet Carbonyls in Biological Systems. *Chemical Research in Toxicology* **2007**, *20*, 1162–1169.

(12) Russell, G. A. Deuterium-isotope Effects in the Autoxidation of Aralkyl Hydrocarbons. Mechanism of the Interaction of Peroxy Radicals. *Journal of the American Chemical Society* **1957**, *79*, 3871–3877.

(13) Di Mascio, P.; Martinez, G. R.; Miyamoto, S.; Ronsein, G. E.; Medeiros, M. H. G.; Cadet, J. Singlet molecular oxygen: Düsseldorf – São Paulo, the Brazilian connection. *Archives of Biochemistry and Biophysics* **2016**, *595*, 161–175.

(14) Bastos, E. L.; Farahani, P.; Bechara, E. J.; Baader, W. J. Four-membered cyclic peroxides: Carriers of chemical energy. *Journal of Physical Organic Chemistry* **2017**, *30*, e3725.

(15) Vacher, M.; Fdez. Galván, I.; Ding, B.-W.; Schramm, S.; Berraud-Pache, R.; Naumov, P.; Ferré, N.; Liu, Y.-J.; Navizet, I.; Roca-Sanjuán, D.; Baader, W. J.; Lindh, R. Chemi- and Bioluminescence of Cyclic Peroxides. *Chemical Reviews* **2018**, *118*, 6927–6974.

(16) Miyamoto, S.; Martinez, G. R.; Medeiros, M. H.; Di Mascio, P. Singlet molecular oxygen generated by biological hydroperoxides. *Journal of Photochemistry and Photobiology B: Biology* **2014**, *139*, 24–33.

(17) Di Mascio, P.; Martinez, G. R.; Miyamoto, S.; Ronsein, G. E.; Medeiros, M. H. G.; Cadet, J. Singlet Molecular Oxygen Reactions with Nucleic Acids, Lipids, and Proteins. *Chemical Reviews* **2019**, *119*, 2043–2086.

(18) Cadenas, E.; Davies, K. J. Mitochondrial free radical generation, oxidative stress, and aging. *Free Radical Biology and Medicine* **2000**, *29*, 222–230.

(19) Belousov, V. V.; Fradkov, A. F.; Lukyanov, K. A.; Staroverov, D. B.; Shakhbazov, K. S.; Terskikh, A. V.; Lukyanov, S. Genetically encoded fluorescent indicator for intracellular hydrogen peroxide. *Nature methods* **2006**, *3*, 281–286.

(20) Niethammer, P.; Grabher, C.; Look, A. T.; Mitchison, T. J. A tissue-scale gradient of hydrogen peroxide mediates rapid wound detection in zebrafish. *Nature* **2009**, *459*, 996–999.

(21) Rác, M.; Křupka, M.; Binder, S.; Sedlářová, M.; Matušková, Z.; Raška, M.; Pospíšil, P. Oxidative Damage of U937 Human Leukemic Cells Caused by Hydroxyl Radical Results in Singlet Oxygen Formation. *PLOS ONE* **2015**, *10*, e0116958.

(22) Bereta, M.; Teplan, M.; Chafai, D. E.; Cifra, M. Biological autoluminescence as a non-invasive monitoring tool for pulsed electric field effects on yeast cells. 2020 XXXIIIrd General Assembly and Scientific Symposium of the International Union of Radio Science. Rome, Italy, 2020; pp 1–3.

(23) Vahalová, P.; Červinková, K.; Cifra, M. Biological autoluminescence for assessing oxidative processes in yeast cell cultures. *Scientific Reports* **2021**, *11*, 10852.

(24) García-Santamarina, S.; Boronat, S.; Hidalgo, E. Reversible Cysteine Oxidation in Hydrogen Peroxide Sensing and Signal Transduction. *Biochemistry* **2014**, *53*, 2560–2580, Publisher: American Chemical Society.

(25) Turell, L.; Zeida, A.; Trujillo, M. Mechanisms and consequences of protein cysteine oxidation: the role of the initial short-lived intermediates. *Essays in Biochemistry* **2020**, *64*, 55–66.

(26) Stadtman, E.; Berlett, B. Fenton chemistry. Amino acid oxidation. *Journal of Biological Chemistry* **1991**, *266*, 17201–17211.

(27) Kehrer, J. P. The Haber–Weiss reaction and mechanisms of toxicity. *Toxicology* **2000**, *149*, 43–50.

(28) Prousek, J. Fenton chemistry in biology and medicine. *Pure and Applied Chemistry* **2007**, *79*, 2325–2338.

(29) Kanti Das, T.; Wati, M. R.; Fatima-Shad, K. Oxidative Stress Gated by Fenton and Haber Weiss Reactions and Its Association With Alzheimer's Disease. *Archives of Neuroscience* **2014**, *2*.

(30) Buettner, G. R.; Czapski, P. G. Ascorbate autoxidation in the presence of iron and copper chelates. *Free radical research communications* **1986**, *1*, 349–353.

(31) Van Wijk, R.; Van Wijk, E. P.; Schroen, Y.; Van der Greef, J. Imaging human spontaneous photon emission: historic development, recent data and perspectives. *Trends Photochem. Photobiol* **2013**, *15*, 27–40.

(32) Ives, J. A.; van Wijk, E. P. A.; Bat, N.; Crawford, C.; Walter, A.; Jonas, W. B.; van Wijk, R.; van der Greef, J. Ultraweak Photon Emission as a Non-Invasive Health Assessment: A Systematic Review. *PLoS ONE* **2014**, *9*, e87401.

(33) Van Wijk, R.; Van Wijk, E. P.; van Wietmarschen, H. A.; Greef, J. v. d. Towards whole-body ultra-weak photon counting and imaging with a focus on human beings: A review. *Journal of Photochemistry and Photobiology B: Biology* **2014**, *139*, 39–46.

(34) Calcerrada, M.; Garcia-Ruiz, C. Human Ultraweak Photon Emission: Key Analytical Aspects, Results and Future Trends – A Review. *Critical Reviews in Analytical Chemistry* **2019**, *49*, 368–381.

(35) He, M.; Sun, M.; van Wijk, E.; van Wietmarschen, H.; van Wijk, R.; Wang, Z.; Wang, M.; Hankemeier, T.; van der Greef, J. A Chinese literature overview on ultraweak photon emission as promising technology for studying system-based diagnostics. *Complementary Therapies in Medicine* **2016**, *25*, 20–26.

(36) Rastogi, A.; Pospíšil, P. Ultra-weak photon emission as a non-invasive tool for monitoring of oxidative processes in the epidermal cells of human skin: comparative study on the dorsal and the palm side of the hand. *Skin Research and Technology* **2010**,

(37) Van Wijk, R.; Kobayashi, M.; Van Wijk, E. P. Anatomic characterization of human ultra-weak photon emission with a moveable photomultiplier and CCD imaging. *Journal of Photochemistry and Photobiology B: Biology* **2006**, *83*, 69–76.

(38) Seo, D.-I.; M. Laager, F.; Young, K.; Chang, H.; So, W.-Y.; Kim, H.-T.; Soh, K.-S.; Song, W. Ultra-weak photon emission during wrist curl and cycling exercises in trained healthy men. *Electromagnetic Biology and Medicine* **2012**, *31*, 122–131.

(39) Laager, F.; Park, S.-H.; Yang, J.-M.; Song, W.; Soh, K.-S. Effects of exercises on biophoton emission of the wrist. *European journal of applied physiology* **2008**, *102*, 463–469.

(40) Van Wijk, R.; Wijk, E. P. An Introduction to Human Biophoton Emission. *Forschende Komplementärmedizin / Research in Complementary Medicine* **2005**, *12*, 77–83.

(41) Van Wijk, E. P.; Van Wijk, R. Multi-Site Recording and Spectral Analysis of Spontaneous Photon Emission from Human Body. *Forschende Komplementärmedizin / Research in Complementary Medicine* **2005**, *12*, 96–106.

(42) Cifra, M.; Van Wijk, E.; Koch, H.; Bosman, S.; Van Wijk, R. Spontaneous ultra-weak photon emission from human hands is time dependent. *Radioengineering* **2007**, *16*, 15.

(43) Kobayashi, M.; Kikuchi, D.; Okamura, H. Imaging of Ultraweak Spontaneous Photon Emission from Human Body Displaying Diurnal Rhythm. *PLoS ONE* **2009**, *4*, e6256.

(44) Cohen, S.; Popp, F. Low-level luminescence of the human skin. *Skin Research and Technology* **1997**, *3*, 177–180.

(45) Cohen, S.; Popp, F. Biophoton emission of the human body. *Journal of Photochemistry and Photobiology B: Biology* **1997**, *40*, 187–189.

(46) Scholkmann, F.; van de Kraats, E.; van Wijk, R.; van Wijk, E.; van der Greef, J. Spatio-temporal dynamics of spontaneous ultra-weak photon emission (autoluminescence) from human hands measured with an EMCCD camera: Dependence on time of day, date and individual subject. *Matters* **2018**,

(47) Zhao, X.; van Wijk, E.; Yan, Y.; van Wijk, R.; Yang, H.; Zhang, Y.; Wang, J. Ultra-weak photon emission of hands in aging prediction. *Journal of Photochemistry and Photobiology B: Biology* **2016**, *162*, 529–534.

(48) Prasad, A.; Balukova, A.; Pospíšil, P. Triplet Excited Carbonyls and Singlet Oxygen Formation During Oxidative Radical Reaction in Skin. *Frontiers in Physiology* **2018**, *9*, 9.

(49) Ou-Yang, H. The application of ultra-weak photon emission in dermatology. *Journal of Photochemistry and Photobiology B: Biology* **2014**, *139*, 63–70.

(50) Gabe, Y.; Takeda, K.; Tobiishi, M.; Kikuchi, S.; Tsuda, K.; Haryuu, Y.; Nakajima, Y.; Inomata, Y.; Nakamura, S.; Murase, D.; Tokunaga, S.; Miyaki, M.; Takahashi, Y. Evaluation of subclinical chronic sun damage in the skin via the detection of long-

lasting ultraweak photon emission. *Skin Research and Technology* **2021**, *27*, 1064–1071, _eprint: https://onlinelibrary.wiley.com/doi/pdf/10.1111/srt.13059.

(51) Inaba, H. Measurement of biophoton from human body. *J Int Soc Life Inf Sci* **2000**, *18*, 448–452.

(52) Prasad, A.; Pospíšil, P. Towards the two-dimensional imaging of spontaneous ultraweak photon emission from microbial, plant and animal cells. *Scientific Reports* **2013**, *3*.

(53) Prasad, A.; Pospišil, P. Two-dimensional imaging of spontaneous ultra-weak photon emission from the human skin: role of reactive oxygen species. *Journal of Biophotonics* **2011**, *4*, 840–849.

(54) Rastogi, A.; Pospíšil, P. Spontaneous ultraweak photon emission imaging of oxidative metabolic processes in human skin: effect of molecular oxygen and antioxidant defense system. *Journal of Biomedical Optics* **2011**, *16*, 096005.

(55) Tsuchida, K.; Kobayashi, M. Ultraviolet A irradiation induces ultraweak photon emission with characteristic spectral patterns from biomolecules present in human skin. *Scientific Reports* **2020**, *10*, 21667.

(56) Tsuchida, K.; Sakiyama, N.; Ogura, Y.; Kobayashi, M. Skin lightness affects ultraviolet A-induced oxidative stress: evaluation using ultraweak photon emission measurement. *Experimental Dermatology* **2022**, *n/a*, _eprint: https://onlinelibrary.wiley.com/doi/pdf/10.1111/exd.14690.

(57) Niggli, H. J. Artificial sunlight irradiation induces ultraweak photon emission in human skin fibroblasts. *Journal of Photochemistry and Photobiology B: Biology* **1993**, *18*, 281–285.

(58) Sakurai, H.; Yasui, H.; Yamada, Y.; Nishimura, H.; Shigemoto, M. Detection of reactive oxygen species in the skin of live mice and rats exposed to UVA light: a research review on chemiluminescence and trials for UVA protection. *Photochemical & Photobiological Sciences* **2005**, *4*, 715–720.

(59) Musumeci, F.; Applegate, L. A.; Privitera, G.; Scordino, A.; Tudisco, S.; Niggli, H. J. Spectral analysis of laser-induced ultraweak delayed luminescence in cultured normal and tumor human cells: temperature dependence. *Journal of Photochemistry and Photobiology B: Biology* **2005**, *79*, 93–99.

(60) Hagens, R.; Khabiri, F.; Schreiner, V.; Wenck, H.; Wittern, K.-P.; Duchstein, H.-J.; Mei, W. Non-invasive monitoring of oxidative skin stress by ultraweak photon emission measurement. II: biological validation on ultraviolet A-stressed skin. *Skin Research and Technology* **2007**, *0*, 071018045710002–???

(61) Khabiri, F.; Hagens, R.; Smuda, C.; Soltau, A.; Schreiner, V.; Wenck, H.; Wittern, K.-P.; Duchstein, H.-J.; Mei, W. Non-invasive monitoring of oxidative skin stress by ultraweak photon emission (UPE)-measurement. I: mechanisms of UPE of biological materials. *Skin Research and Technology* **2008**, *14*, 103–111.

(62) Kobayashi, M. Highly sensitive imaging for ultra-weak photon emission from living organisms. *Journal of Photochemistry and Photobiology B: Biology* **2014**, *139*, 34–38.

(63) Tsuchida, K.; Iwasa, T.; Kobayashi, M. Imaging of ultraweak photon emission for evaluating the oxidative stress of human skin. *Journal of Photochemistry and Photobiology B: Biology* **2019**, *198*, 111562.

(64) Martínez-Garay, C. A.; de Llanos, R.; Romero, A. M.; Martínez-Pastor, M. T.; Puig, S. Responses of Saccharomyces cerevisiae Strains from Different Origins to Elevated Iron Concentrations. *Applied and Environmental Microbiology* **2016**, *82*, 1906–1916.

(65) Olivieri, N. F. Progression of iron overload in sickle cell disease. *Seminars in Hematology* **2001**, *38*, 57–62.

(66) Wood, J. C. Estimating Tissue Iron Burden: Current Status and Future Prospects. *British journal of haematology* **2015**, *170*, 15–28.

(67) Meyerstein, D. What Are the Oxidizing Intermediates in the Fenton and Fenton-like Reactions? A Perspective. *Antioxidants* **2022**, *11*, 1368.

(68) Garcia, D. A fast all-in-one method for automated post-processing of PIV data. *Experiments in Fluids* **2010**, *50*, 1247–1259, Publisher: Springer Science and Business Media LLC.

(69) Garcia, D. Robust smoothing of gridded data in one and higher dimensions with missing values. *Computational Statistics & Data Analysis* **2010**, *54*, 1167–1178.

(70) *MATLAB version 9.10.0.1602886 (R2021a)*; The Mathworks, Inc.: Natick, Massachusetts, 2021.

(71) Kobayashi, M.; Iwasa, T.; Tada, M. Polychromatic spectral pattern analysis of ultraweak photon emissions from a human body. *Journal of Photochemistry and Photobiology B: Biology* **2016**, *159*, 186–190.

(72) Pappas, A.; Johnsen, S.; Liu, J.-C.; Eisinger, M. Sebum analysis of individuals with and without acne. *Dermato-Endocrinology* **2009**, *1*, 157–161.

(73) Picardo, M.; Ottaviani, M.; Camera, E.; Mastrofrancesco, A. Sebaceous gland lipids. *Dermato-Endocrinology* **2009**, *1*, 68–71.

(74) de Paulet, A. C., Douste-Blazy, L., Paoletti, R., Eds. *Free Radicals, Lipoproteins, and Membrane Lipids*; Springer US: Boston, MA, 1991.

(75) Ref. 74, Ch 1.

(76) Banerjee, A. K.; Mandal, A.; Chanda, D.; Chakraborti, S. Oxidant, antioxidant and physical exercise. *Molecular and cellular biochemistry* **2003**, *253*, 307–312.

(77) Repetto, M.; Semprine, J.; Boveris, A. In *Lipid Peroxidation*; Catala, A., Ed.; InTech, 2012.

(78) Vahalová, P.; Havelka, D.; Vaněčková, E.; Zakar, T.; Kolivoška, V.; Cifra, M. Biochemiluminescence Sensing of Protein Oxidation by Reactive Oxygen Species Generated by Pulsed Electric Field. 2023; `https://papers.ssrn.com/abstract=4328202`.

(79) Loo, A. E. K.; Ho, R.; Halliwell, B. Mechanism of hydrogen peroxide-induced keratinocyte migration in a scratch-wound model. *Free Radical Biology and Medicine* **2011**, *51*, 884–892.

(80) Finlayson, L.; Barnard, I. R. M.; McMillan, L.; Ibbotson, S. H.; Brown, C. T. A.; Eadie, E.; Wood, K. Depth Penetration of Light into Skin as a Function of Wavelength from 200 to 1000 nm. *Photochemistry and Photobiology* **2022**, *98*, 974–981, _eprint: https://onlinelibrary.wiley.com/doi/pdf/10.1111/php.13550.

(81) Tsuchida, K.; Sakiyama, N. Blue light-induced lipid oxidation and the antioxidant property of hypotaurine: evaluation via measuring ultraweak photon emission. *Photochemical & Photobiological Sciences* **2022**,

TOC Graphic